

INDUCTION HEATING OF ROTATING NONMAGNETIC BILLET IN MAGNETIC FIELD PRODUCED BY HIGH-PARAMETER PERMANENT MAGNETS

Обсуждается и моделируется прогрессивный метод индукционного нагрева немагнитных заготовок. Заготовка вращается в стационарном магнитном поле, создаваемом неподвижными высококоэрцитивными постоянными магнитами, закрепленными на магнитопроводе соответствующей формы. Математическая модель задачи, состоящая из двух связанных дифференциальных уравнений в частных производных, решается численно в "жесткой" постановке. Вычисления выполняются с использованием собственного программного обеспечения Agros2D на основе полностью адаптивного метода конечных элементов высоких порядков. Наиболее важные результаты подтверждены экспериментально на собственном лабораторном оборудовании.

An advanced way of induction heating of nonmagnetic billets is discussed and modeled. The billet rotates in a stationary magnetic field produced by unmoving high-parameter permanent magnets fixed on magnetic circuit of an appropriate shape. The mathematical model of the problem consisting of two coupled partial differential equations is solved numerically, in the monolithic formulation. Computations are carried out using our own code Agros2D based on a fully adaptive higher-order finite element method. The most important results are verified experimentally on our own laboratory device.

INTRODUCTION

Induction heating of nonmagnetic billets (mostly of aluminum) belongs to widespread heat treatment technologies applied before their hot forming [1]. To the date, three basic modifications of the process have been introduced in the industrial plants.

The oldest way is heating of an unmoving billet in a system of one or more harmonic or periodic current-carrying inductors (see Fig. 1).

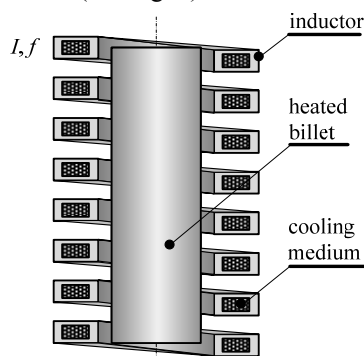


Fig. 1. Classical induction heating of billet in inductor carrying harmonic current of amplitude I and frequency f

Unfortunately, the efficiency of this way is rather low (reported values mostly do not exceed about 45 %), mainly due to high Joule losses in the inductor. More information can be found, for example, in [2-4].

Another technology introduced much later consists in rotation of a billet in static magnetic field produced by one or more longitudinal turns carrying direct current (see Fig. 2).

This way of heating, however, requires a very high magnetic field in order to obtain sufficiently high currents induced in the billet and corresponding Joule losses. This means very high field currents available only in superconducting systems. The Joule losses are now very low, but certain amount of energy is consumed by the cooling devices and for surpassing the drag electromagnetic torque. Presently, such systems work in few industrial plants, but their cost is high and reliability is rather poor. The efficiency is about 70 %. Fig. 3 shows a typical device of this kind at Weseralu (Germany) [5].

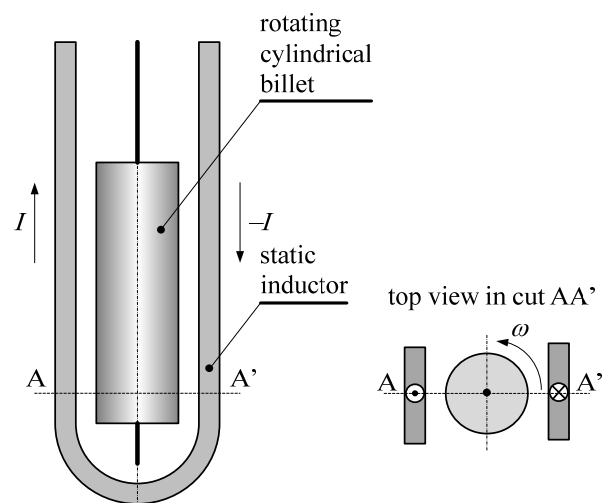


Fig. 2. Billet rotating in static magnetic field produced by direct-current carrying coil



Fig. 3. Induction heating of billet rotating in superconducting system (Weseralu, Germany, 2009)

In years 2009-2010, a new way of induction heating of the billets was suggested and investigated (Finland, Italy, Germany, Czech Republic), namely in static magnetic field produced by a system of high-parameter permanent magnets, see Fig. 4. The arrangement is characterized by the absence of Joule losses and its efficiency exceeds 80 %.

A year later, an inverse version of the system indicated in Fig. 4 was proposed, intended for heating billets of larger radii: a well dynamically balanced ring with permanent magnets rotates around an unmoving billet. Construction of such a system, however, is more complicated from the technological point of view.

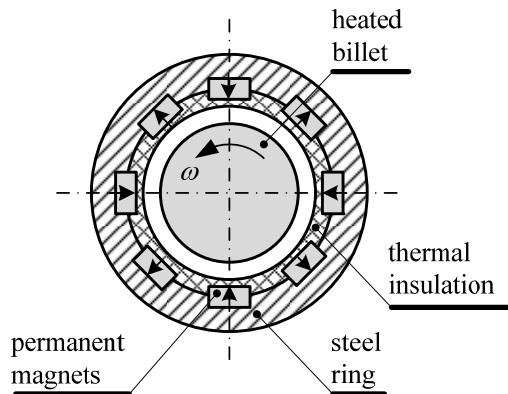


Fig. 4. Billet rotating in static magnetic field produced by high-parameter permanent magnets

FORMULATION OF TECHNICAL PROBLEM

In 2011, after a long testing and evaluating process we decided to build an experimental device for heating billets up to diameter of 60 mm. The device is depicted in Fig. 5. It consists of an induction motor driving the billet and an active part consisting of a massive magnetic circuit with fixed high-parameter permanent magnets. The cross section of the active part, together with its principal dimensions in mm, is shown in Fig. 6.

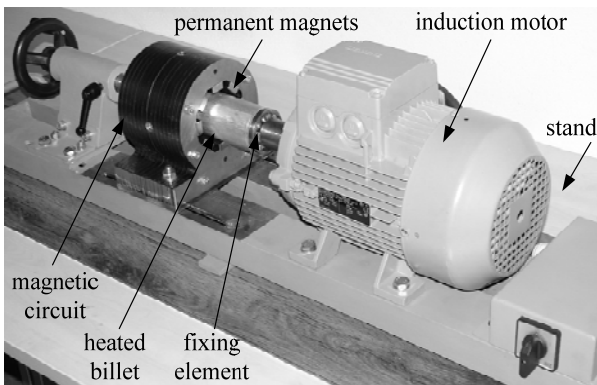


Fig. 5. View of laboratory device

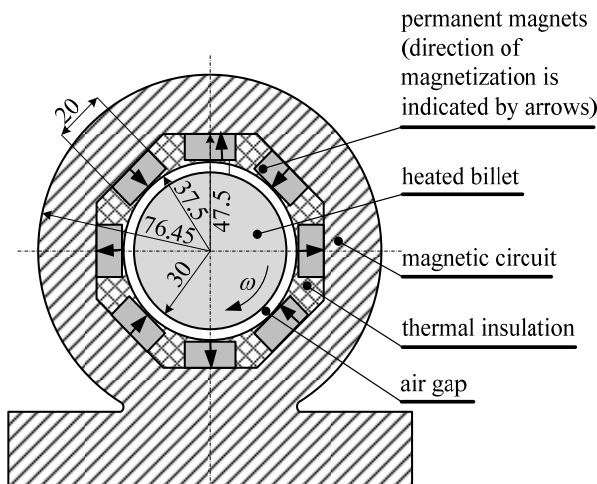


Fig. 6. Cross section of active part of laboratory device

The paper presents the complete continuous mathematical model that is solved numerically in the monolithic formulation and comparison of the most important results with relevant experimental data measured on the above model.

CONTINUOUS MATHEMATICAL MODEL

The problem is characterized by an interaction of two physical fields: magnetic field and temperature field. The volume changes of the billet due to its temperature rise are insignificant in this case and may be neglected.

Magnetic field can conveniently be described in terms of the magnetic vector potential A . Its distribution in the investigated system is given by the equation [6]

$$\text{curl} \left(\frac{1}{\mu} (\text{curl} A - \mathbf{B}_r) \right) - \gamma \mathbf{v} \times \text{curl} A = 0, \quad (1)$$

where μ is the magnetic permeability (in ferromagnetic materials permeability $\mu = \mu(B)$, B being the module of the magnetic flux density), \mathbf{B}_r denotes the remanent magnetization (that is only considered in the permanent magnets, otherwise it vanishes), γ stands for the electric conductivity and \mathbf{v} represents the vector of the local velocity of rotation.

The definition area is surrounded by a sufficiently distant boundary described by the Dirichlet condition $A = 0$.

The distribution of temperature field T in the system is described by the heat transfer equation [7]

$$\text{div}(\lambda \text{grad} T) - \rho c_p \left(\frac{\partial T}{\partial t} + \mathbf{v} \cdot \text{grad} T \right) = -w, \quad (2)$$

where λ denotes the thermal conductivity, ρ is the specific mass, and c_p represents the specific heat at a constant pressure. The equation is time-dependent. The source term w stands for the volumetric heat generated in the material by the Joule and/or magnetization losses. Its value is generally given by the sum of the volumetric Joule losses w_J and volumetric magnetization losses (in ferromagnetic materials) w_m . Here,

$$w_J = \frac{1}{\gamma} |\mathbf{J}_{ind}|^2, \quad \mathbf{J}_{ind} = \gamma \mathbf{v} \times \text{curl} A, \quad (3)$$

while the magnetization losses must be determined from the loss curves of the corresponding material or using an appropriate approximate (for example Steinmetz) formula.

The boundary condition respects the heat convection and may generally be expressed by the formula

$$-\lambda \frac{\partial T}{\partial n} = \alpha(T - T_{ext}) + \sigma C(T^4 - T_r^4), \quad (4)$$

where n represents the direction of the outward normal to the surface of the volume in which heat is produced, α denotes the coefficient of convection, T_{ext} is the average temperature of ambient air, $\sigma = 5.67073 \cdot 10^{-8} \text{ Wm}^{-2}\text{K}^{-4}$ is the Stefan-Boltzmann constant, C denotes the coefficient of emissivity (and may also include the influence of the multiple reflections or configuration factor) and, finally, T_r represents the temperature of the reflecting surface.

Unfortunately, in most cases, the coefficients α and C occurring in boundary condition (4), cannot be determined accurately. That is why we use instead of (4) a simplified condition

$$-\lambda \frac{\partial T}{\partial n} = \alpha_{gen}(T - T_{ext}), \quad (5)$$

where α_{gen} represents a generalized coefficient of the convective heat transfer respecting also the heat losses in the fronts of the active parts of the arrangement. This coefficient has to be usually determined by means of specific measurements.

NUMERICAL SOLUTION

The material parameters are considered to be temperature-dependent functions. This is an important reason why the system must be solved in the hard-coupled formulation (monolithically); otherwise one could not avoid inaccuracies typical for the weakly coupled approach.

On the other hand, such a system of nonlinear and nonstationary PDEs in a 3D domain is still practically insolvable by the available means; the main reason is a relatively long time of heating (on the order of minutes). That is why a few simplifying assumptions had to be accepted:

- the arrangement is considered sufficiently long in the axial direction, so that both magnetic and temperature fields are calculated only in its cross section, as is depicted in Fig. 4. This means that the task is solved as a 2D problem;

- both computations and experiments confirmed that the temperatures of magnetic circuit and permanent magnets remain relatively low (they not exceed about 65 °C). The material properties of the ferromagnetic ring and permanent magnets, therefore, can be considered independent of the temperature.

The numerical solution itself was carried out by our own code. This code called Agros2D [8] cooperating with the library Hermes [9] is based on a fully adaptive higher-order finite element method [10]. Both the codes written in C++ are intended for the numerical solution of systems of generally nonlinear and nonstationary second-order partial differential equations (PDEs) and their principal purpose is to model complex physical phenomena. They are freely distributable under the GNU General Public License. Mentioned should be some of their unique features such as:

- solution of a system of PDEs may be solved in both weakly coupled and hard-coupled formulations. In the latter case the resultant numerical scheme is characterized by just one stiffness matrix;

- there are three kinds of the adaptive algorithms implemented in the code. Except for more common h -adaptivity and p -adaptivity, also the most sophisticated hp -adaptivity may be used;

- each of the mapped physical fields can be solved on a quite different mesh. For example, the temperature field is often highly smooth, so that it is not necessary to solve it on an unnecessarily dense mesh (such as in case of the magnetic fields). As far as the task is nonstationary, the meshes can evolve in time according to the results obtained in the previous step;

- the codes can work with the hanging nodes of any level, which leads to a substantial reduction of the degrees of freedom (DOFs);

- besides classical triangles, the codes are able to mix even quadrilateral and curved elements. The curved elements are very advantageous for accurate modeling curvilinear boundaries and interfaces.

ILLUSTRATIVE EXAMPLE

The methodology was used for mapping the process of induction heating of an aluminum billet of diameter 60 mm. The principal dimensions of the arrangement (in mm) are shown in Fig. 6. Its axial length is 300 mm.

Input Data:

- magnetic circuit: made of carbon steel CSN 12 040 of the Czech make (its magnetization characteristic being depicted in Fig. 7). As its temperature is low during the process, its magnetic permeability is considered temperature-independent.

- The permanent magnets VMM10 are of NdFeB type and their manufacturer provides the following parameters: remanence $B_r = 1.45$ T, relative permeability in the second quadrant $\mu_r = 1.21$ and maximum allowable temperature is 80 °C. Their dimensions are 10×20×40 mm.

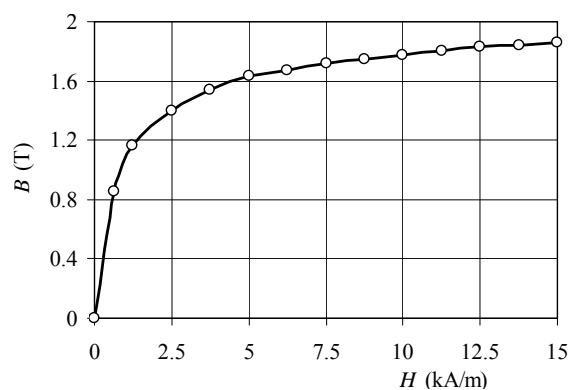


Fig. 7. Magnetization characteristic of steel CSN 12 040

- The thermal insulation is glass wool of very poor thermal conductivity ($\lambda = 0.12$ Wm⁻¹K⁻¹). Except for the front effects, the process of heating of the billet is then almost adiabatic (which was also confirmed both computationally and experimentally).

- Aluminum billet: as its manufacturer was not able to guarantee its exact chemical composition, its properties are described by the temperature-dependent parameters for pure aluminum. These are depicted in Figs. 8-10 (see [11]).

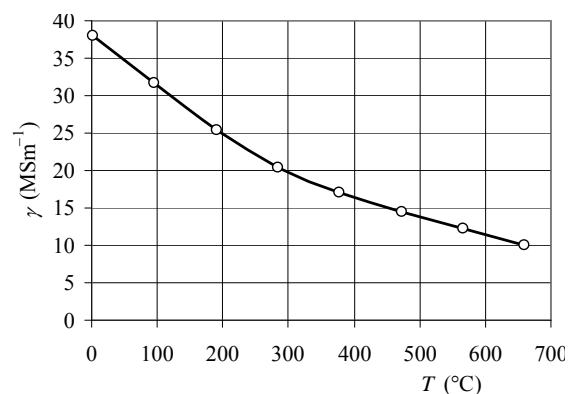


Fig. 8. Electric conductivity γ versus temperature T for pure Al

The principal parameters of the three-phase induction motor are as follows: $P = 3$ kW, $\cos \varphi = 0.82$, $n_{\text{nom}} = 1420$ rpm, $U = 230/400$ V. The initial temperature of the billet before heating (as well as the temperature of ambient air) $T_0 = 20$ °C.

A very complicated business was determination of the exact value of the coefficient α_{gen} , mainly because of the velocity of rotation, configurations factors, multiple reflections and surface properties. That is why this value was found using the experimental calibration consisting in the requirement that the calculated and measured surface temperatures of the billet are in the closest possible rela-

tion. In this way we obtained $\alpha_{gen} = 125 \text{ Wm}^{-2}\text{K}^{-1}$, which respects all above items.

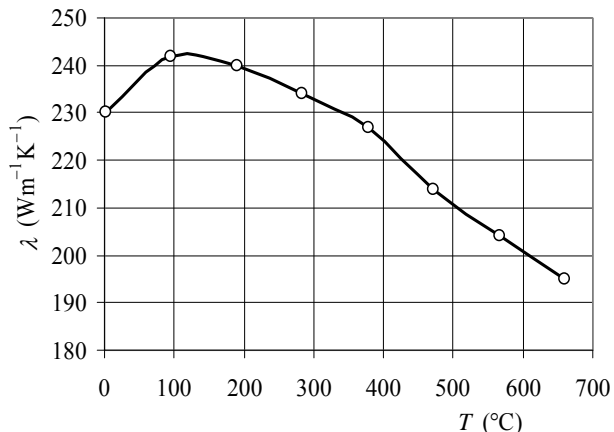


Fig. 9. Thermal conductivity λ versus temperature T for pure Al

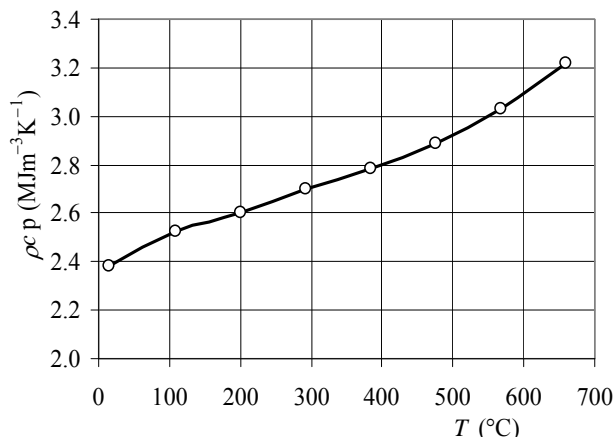


Fig. 10. Heat capacity ρc_p versus temperature T for pure Al

Results:

Fig. 11 shows a substantial part of the discretization mesh covering the active area (at the end of the process of adaptivity) used for computation of magnetic field in the system. The numbers in the rectangles denote the degrees of polynomials in particular elements.

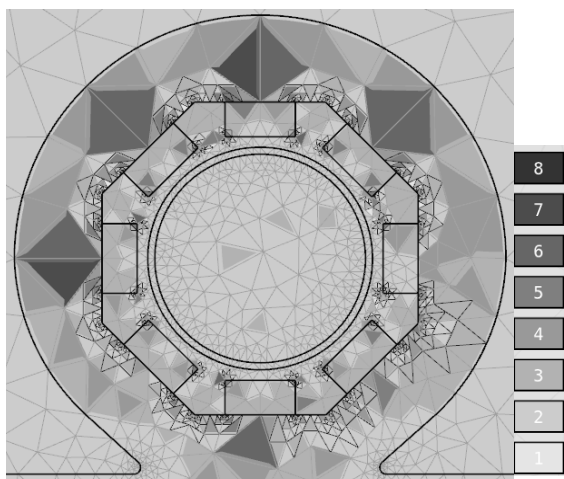


Fig. 11: Discretization mesh: light lines – before adaptivity, dark lines – after adaptivity, numbers in right column show orders of corresponding elements)

The billet is discretized using the triangular and curvilinear elements. The regions in the neighborhood of the

corners of the magnetic circuit representing the singular points are discretized by small triangles of low polynomial orders while places with expected smooth regions are covered by large triangles of high polynomial orders.

Fig. 12 shows the distribution of volumetric Joule losses w_j produced by the currents induced in the rotating billet. In accordance with theory, the highest (both positive and negative) values are generated in the surface layers of the billet.

Fig. 13 shows the distribution of temperature in the billet after 180 s of heating. The temperatures over its whole cross section do not differ more than by a few degrees of centigrade. This is caused by a very good thermal conductivity of aluminum.

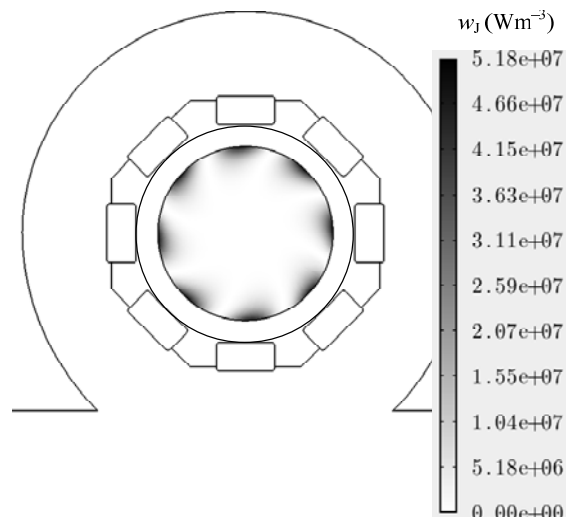


Fig. 12. Volumetric Joule losses w_j in billet at beginning of process of heating

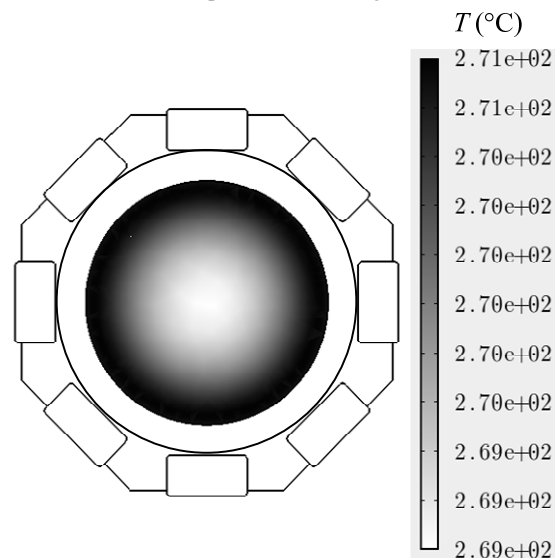


Fig. 13. Distribution of temperature T in billet after 180 s of heating for $n_{nom} = 1420 \text{ rpm}$

Fig. 14 compares the calculated and measured curves of the temperature evolution in the center and on the external surface of the billet. It is evident that the agreement is extremely good.

Another important quantity characterizing the process of heating is its efficiency η . Its value was both measured and calculated. The experimental value was determined as the ratio

$$\eta = \frac{Q_T}{\int_0^{t_{\max}} P_L dt}, \quad (6)$$

where Q_T denotes the heat used for the increase of temperature of the billet and P_L is the active power delivered to the loaded induction motor. Both values of P_L and Q_T are temperature-dependent. Symbol t_{\max} denotes the time of heating. The total active power was measured in all phases by a network analyzer. It decreases with time, because the electric conductivity of the billet decreases with temperature, which leads to subsequent decrease of the induced currents, heat power and also electromagnetic drag torque acting on the billet (see Fig. 15).

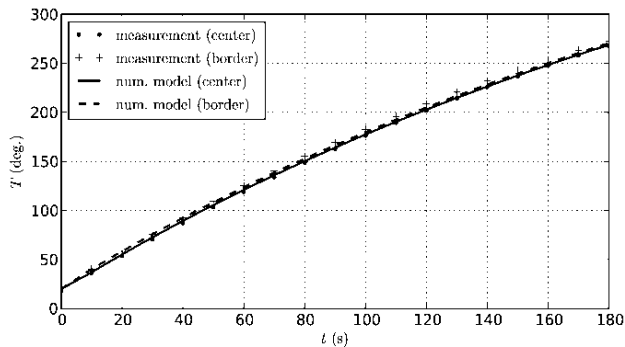


Fig. 14. Comparison of measured and calculated time evolutions of temperature in axis and on surface of billet

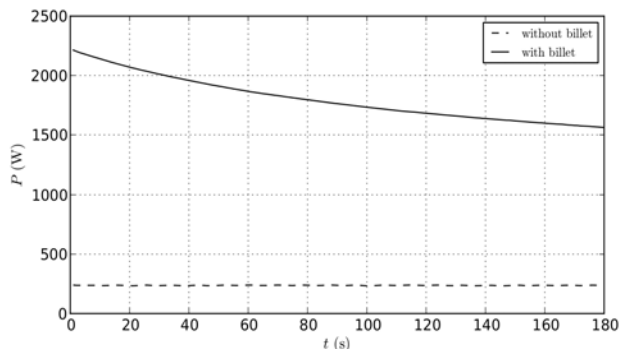


Fig. 15. Measured time evolutions of total active powers of loaded motor and unloaded motor

The heat Q_T can be determined from the formula

$$Q_T = \int_V \rho c_p (T - T_0) dV, \quad (7)$$

where T is the distribution of the final temperature of the billet after ending the heating process and V denotes the volume of the billet. Both measurements and computation provide $\eta = 78 \%$, which is much more in comparison with the classical process.

CONCLUSION

The paper present an alternative way of induction heating of nonmagnetic cylindrical billets consisting in their rotation in static magnetic field generated by high-parameter permanent magnets. The process is modeled and the model is numerically solved by own code based on a fully adaptive higher-order finite element method.

The principal results were verified on an experimental stand built in our laboratory that allows processing billets up to diameter 60 mm. The comparison between

the measurements and simulations is very good and confirms a high efficiency of the process.

Next work in the area will be aimed at the analysis of further possibilities of increasing efficiency of the process. Investigated will be also an inverse solution of the arrangement with unmoving billet and a ring with permanent magnets rotating around it (which will be built in near future).

ACKNOWLEDGMENT

Financial support of the Grant project GACR P102/11/0498 is highly appreciated.

REFERENCES

1. Rudnev V., Loveless D., Cook R., Black M. *Handbook of Induction Heating*. Marcel Dekker, Inc., New York, 2003.
2. Chaboudez C., Clain S., Glardon R., Mari D., Rappaz J., Swierkosz M. Numerical modeling in induction heating for axisymmetric geometries. *IEEE Trans. Magn.*, 1997, vol.33, no.1, pp. 739-735.
3. Nerg J., Partanen J. Numerical solution of 2D and 3D induction heating problems with non-linear material properties taken into account. *IEEE Trans. Magn.*, 1999, vol.35, no.3, pp. 720-722.
4. Jang J.Y., Chiu Y.W. Numerical and experimental thermal analysis for a metallic hollow cylinder subjected to step-wise electro-magnetic induction heating. *Applied Thermal Engineering*, 2007, vol.27, pp. 1883-1894.
5. Available at: <http://www.weseralu.de> (accessed 9 May 2012).
6. Kuczmann M., Iványi A. *The Finite Element Method in Magnetics*. Akadémiai Kiadó, Budapest, 2008.
7. Holman J.P. *Heat Transfer*. McGraw-Hill, New York, 2002.
8. Karban P. and others. *Multiplatform C++ application for the solution of PDEs*. Available at: <http://agros2d.org> (accessed 15 May 2013).
9. Solin P. and others, *Hermes-Higher-order modular finite element system (User's guide)*. Available at: <http://hpfem.org/> (accessed 19 October 2012).
10. Solin P., Segeth K., Dolezel I. *Higher-Order Finite Element Methods*, CRC Press, Boca Raton, FL, USA, 2003.
11. *Temperature dependent elastic and thermal properties database*. Available at: <http://www.jahm.com> (accessed 2 May 2013).

Received 09.10.2013

Ivo Doležel¹, Professor,

Pavel Karban², Associate Professor,

Frantisek Mach², Ph.D. Student,

¹ Czech Technical University, Academy of Sciences of the Czech Republic (Institute of Thermomechanics),

Technická 2, 182 00 Praha 8, Czech Republic,

e-mail: dolezel@fel.cvut.cz

² University of West Bohemia,

Univerzitní 26, 306 14 Plzeň, Czech Republic,

e-mail: karban@fel.zcu.cz, fmach@kte.zcu.cz

Key words – induction heating in rotation, monolithic model, higher-order finite element method, magnetic field, temperature field.